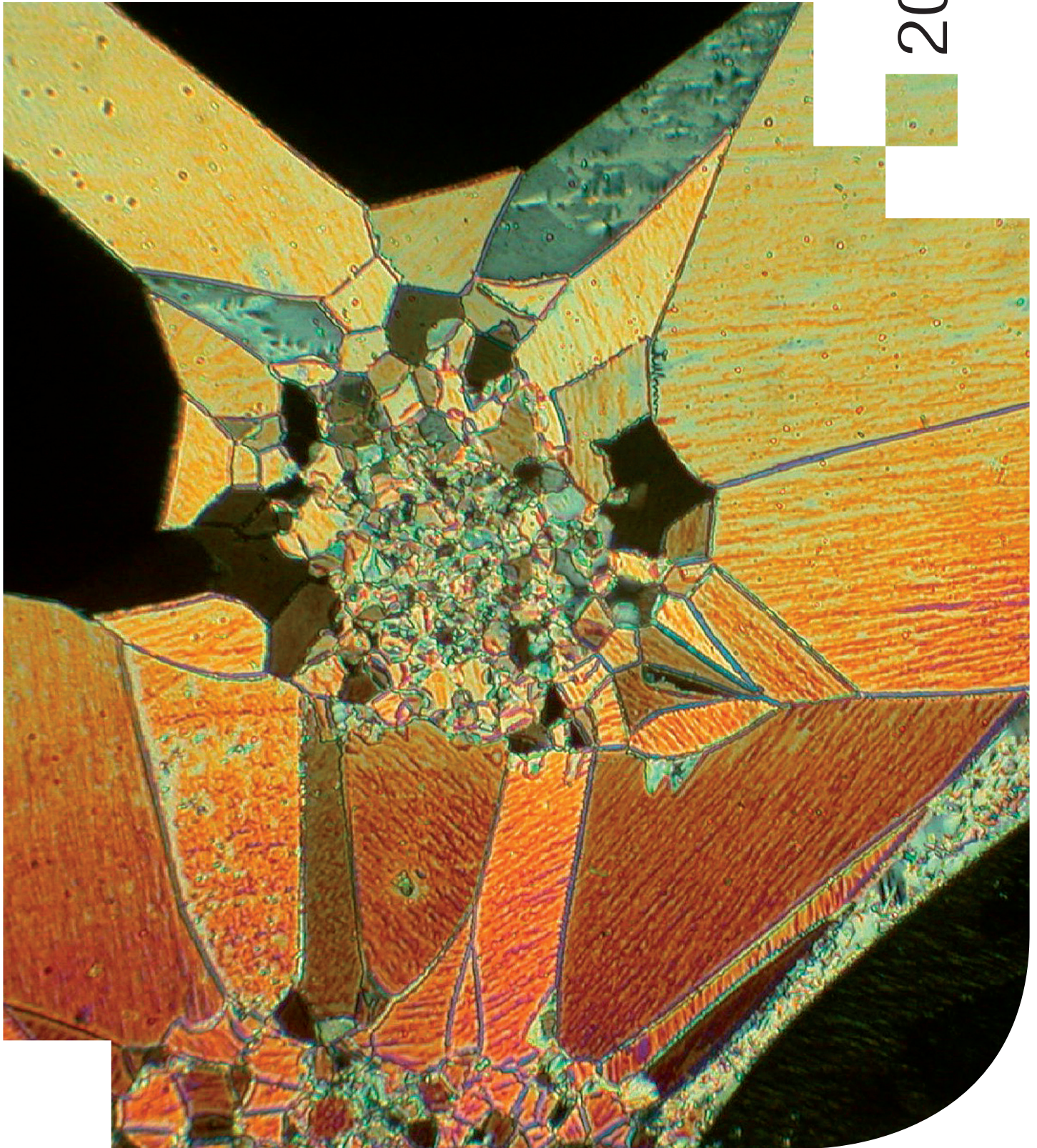


XMas

NEWSLETTER

2014



CONTENTS

3 Facility News

4 Condensed Matter

6 Surfaces & Interfaces

8 Soft Matter

11 Energy

12 Healthcare

13 Cultural Heritage

14 Facility Information

15 Guidelines

The XMaS beamline is now over two years into its operation as an EPSRC mid-range facility. During the first two years we have provided nearly 900 experimental shifts with an average up-time of over 96%. We were pleased to receive a record number of applications for beamtime in the last round of 2014 covering an ever broader range of materials science. Full details of our statistics and performance metrics can be found on: <http://www.xmas.ac.uk>

We welcome any comments and/or feedback you have and will continue to strive to enhance and develop the facility. The latest upgrade to the ESRF is a replacement of the magnetic lattice with a major shut-down beginning in 2018. The major impact for XMaS is that our current bending magnet source will be replaced by a multipole Wiggler. This exciting development will ensure that we can continue to provide our current portfolio as well as opening up a number of opportunities which will radically upgrade the capabilities and capacities of the beamline. In preparation for the upgrade program we are putting together a technical design review as well as developing a science case for the beamline post 2017. Four themed workshops, where we sought the views of a wide range of users and other interested parties, took place in November 2014 to begin this process. We will keep you informed of the progress we are making through the website and at the user meeting in June.

In terms of technical developments, we are pleased to report that our “off-line” facilities, that make wider use of the capital equipment that already exists, are now becoming available for users. These include a laboratory-based x-ray micro-source equipped with a diffractometer that is compatible with many of our sample environments used on the beamline. The reconditioned diffractometer coupled to a new x-ray source is currently being commissioned and will be available for users from late spring 2015. It will be useable both for pre-alignment of samples prior to synchrotron beamtime and for “stand-alone” experiments. In addition, the facility for the measurement of electrical properties is now being sited in a new purpose-built laboratory close to the beamline. There are funds to support users to make use of these facilities. Details of the access mechanisms

for the offline facilities can be found on the website. A range of new detectors are now available on the beamline, including both Maxipix and Pilatus 300K pixel detectors. If you have an idea for an experiment that can make use of the XMaS beamline, but requires some additional instrumental development in terms of sample environment then please don't hesitate to contact us, as funds may be available to help realise such projects.

One of our main collaborative projects, the Nanostrain EURAMET project in partnership with the National Physical Laboratory is now up and running and has already yielded some important new results and outreach publications (<http://www.piezoinstitute.com/resources/emrp-nanostrain/>). In August 2014 we welcomed Sean McMitchell to a postdoctoral research position as part of this project. Sean has an excellent track record in multiferroic materials research and in addition to his primary role in the Nanostrain project, he will be a valuable member of the beamline team.

We have helped to support and organise several meetings over the past year. These include “Surface Science with Synchrotron Radiation”, “New possibilities in x-ray absorption spectroscopy between 2 & 4 keV”, “Latest Developments in Frustrated Magnetism” and “Preserving our history: Cultural heritage and the science behind it”. If you would like us to help organise a focused event covering any current or future opportunities on XMaS, please get in touch as we have some funds available for these activities. In June 2014 the XMaS Annual User Meeting was held at the University of Warwick and was attended by ~50 scientists with 10 user presentations spanning the range of science performed at the beamline. In May 2015, the user meeting will take place at the University of Liverpool - check the XMaS website for more details.

As part of the wider reorganisation of the ESRF main hall, we are happy to announce that the beamline staff offices are now located in close proximity to the beamline. The offices are located on the mezzanine level in the area of the old XMaS PLUO now replaced by the Chartreuse Experimental Hall.

Finally, congratulations to Laurence Bouchenoire on the birth of her baby girl, Coralie.

Chris Lucas, Tom Hase and Malcolm Cooper

On the cover: Crossed polariser optical micrograph showing the ribbon phase of bundled thermotropic bolapolyphiles (see article p 9).

Offline facilities

As we write this article, the new offline x-ray lab source from AXO Dresden GmbH is being installed (**Fig. 1**). During the previous few months, a lead cabin, which houses this x-ray system and beamline personal safety system (PSS) have been installed at the end of the beamline. By using a standard ESRF PSS safety system, any user who has performed the ESRF online safety training will be permitted to use this new lab source. A Huber 4-circle diffractometer has also been completely refurbished and is currently being installed on site. This diffractometer has an identical Eulerian cradle to the main XMaS diffractometer and most of the sample environments available on the main instrument can be used with it. During the early part of the New Year, the facility will be commissioned and made available to the XMaS user community.

During the first few months of the New Year, the beamline will be acquiring some new lab space opposite the end of the beamline. This space will primarily be used for sample preparation and also offline electrical characterisation measurements, such as PE loops and resistivity as a function of temperature and magnetic field. The lab is currently being refurbished and will hopefully be available for use in the spring of 2015.

A wiggler for a bending magnet

Continuing from the ESRF Upgrade Programme Phase I (2009-2015), where 19 public beamlines and end stations are under complete reconstruction or major refurbishment, the proposal for Upgrade Programme Phase II (2015-2022) is at an advanced stage and a Technical Design Study has been produced for the consideration of ESRF Council. The plan is to carry out a major upgrade of the storage ring lattice, in the period 2015-2020, to dramatically reduce the emittance of the source, together with the construction of four new ID beamlines to fully exploit the brilliance and coherence properties of the new source in the period 2020-2022.

For current bending magnet (BM) beamlines, although there are options to remain with BM sources of limited horizontal aperture and magnetic field, the preferred option is a short three pole wiggler (3PW). This change in the sources represents a major enhancement in the flexibility of ESRF BM beamlines. With the current lattice the BM sources are in integral parts of the storage ring and cannot be changed in any way without disturbing the

operation of the ring. With the new lattice, however, only the available length restricts the configuration of the wigglers which could be inserted.

The major advantages for XMaS will be an increased flux at higher energies and a reduced focal spot size. The energy range at XMaS is currently ~2 to 15 keV, with the upper limit set by the cut-off of the toroidal mirror. By changing this optical element, perhaps to a double toroid, it is envisaged that after the upgrade, the upper limit for focused beam operation could be as high as ~50 keV through use of the Si(333) reflection of the monochromator. Unfocused beam up to 100 keV may also be possible.

In order to evaluate interest in this development from the UK scientific community, four meetings were held in November. These were divided into Hard Condensed Matter, Chemistry and EXAFS, Surface and Electrochemistry and Soft Condensed Matter and GISAXS. All of these meetings concluded that it was desirable to exploit the potential for higher energies and a detailed summary of the outcomes can be found on our beamline web pages.

As a result of these meetings, we are now in the process of developing a detailed technical design study to facilitate the scientific case and provide a 2020 vision for XMaS. These will form the basis of our next statement of need for funding and will highlight how XMaS will become a unique and novel synchrotron facility capable of performing both low and high energy measurements on the same sample in a single experimental run.



Fig. 1: The new offline x-ray lab during source (far right of image) installation.

Dynamic in-situ electrical and interferometry measurement capability with high resolution x-ray diffraction synchronisation

C. Vecchini, P. Thompson, M. Stewart, A. Muniz-Piniella, J. Wooldridge, S. McMitchell, S. Lepadatu, L. Bouchenoire, S. D. Brown, D. Wermelle, O. Bikondoa, C. Lucas, T. Hase, M. Cain – for more information contact C. Vecchini, National Physical Laboratory, Hampton Road, Teddington, TW11 0LW, UK.

carlo.vecchini@npl.co.uk

With the US electronics giant IBM having recently filed the first patents for piezoelectric transistors, European physicists, materials scientists and metrologists have joined forces in a project called Nanostrain to develop the metrology and the understanding necessary to drive innovation and enable the development of novel electronic devices based on the control of strain at the nano scale [1]. As part of this collaborative project, the UK National Physical Laboratory and the XMaS beamline team have worked closely together to combine very different techniques into a unique capability now in operation at the XMaS beamline (Fig. 2). X-ray diffraction, which is used to measure crystallographic changes at the atomic level, and optical interferometry, to measure displacement, have been coupled at the XMaS beamline. This new facility has been incorporated with the recently developed [2] in-situ/in-operando capability to apply an AC electric field to the specimen of interest and, if ferroelectric, measure the electrical polarization. This comprehensive system for strain characterization in single crystals and thin films enables scientist to investigate different strain components as functions

of external stimuli (electric field amplitude, frequency, phase, duration, waveform, etc...) working at different lengths scales: from micrometre displacements (global strain) to hundreds of femtometers (atomic strain) as well as the possibility to explore different device geometries and electrode configurations. The combined information (Fig. 3) allows new insights to be gleaned on the correlation between induced strain and material properties, information of crucial importance for the development of novel devices such as IBM's patented Piezoelectric Effect Transistor. This new capability was commissioned at the XMaS beamline in March 2014, with the first experiments performed in July 2014. The success of the integration has been proven with the observation of interferometrically measured displacements down to 50 picometers, which, when combined with 10^{-4} Angstroms lattice displacements measured with x-rays, provides an unprecedented and comprehensive level of information. Measurement challenges and alignment issues have been addressed by identifying the best measurement practices and incorporating them into the control software for a more user friendly facility. After this initial success, the next step will be the development of a complex sample environment to allow for temperature, electric and magnetic field applications to be investigated, and last but not least, the system will be upgraded and pushed into the MHz frequency domain. This will be a crucial step in enabling the understanding of materials and devices near real operational conditions: AC control fields and >MHz frequencies.

[1] www.nanostrain.eu.

[2] Wooldridge *et al.*, J. Synchrotron Rad. 19, 710 (2012).

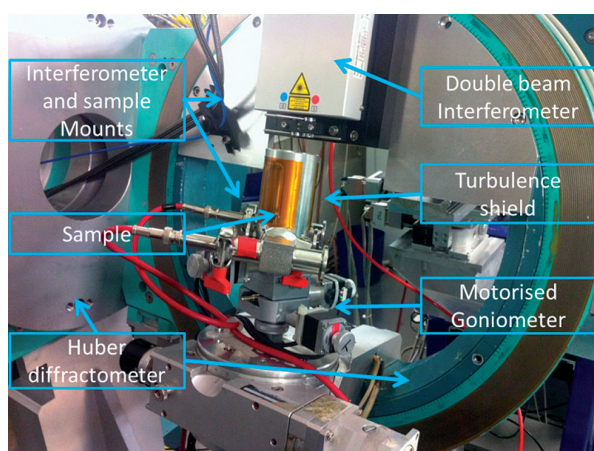


Fig. 2: Interferometer and newly designed sample holder fitted onto the XMaS Huber diffractometer.

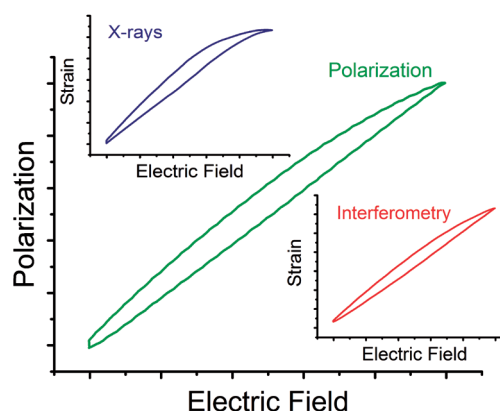


Fig. 3: Simultaneous acquisition of the dynamic response of a ferroelectric material: electrical polarization (green), strain calculated from *d*-spacing (X-rays, blue) and displacement (Interferometry, red).

Measuring the Dzyaloshinskii–Moriya interaction in a weak ferromagnet

V. E. Dmitrienko, E. N. Ovchinnikova, S. P. Collins, G. Nisbet, G. Beutier, Y. O. Kvashnin V. V. Mazurenko, A. I. Lichtenstein, M. I. Katsnelson – for more information contact S. P. Collins, Diamond Light Source Ltd, Diamond House, Harwell Science and Innovation Campus, Didcot, Oxfordshire, OX11 0DE, UK.

steve.collins@diamond.ac.uk

The Dzyaloshinskii–Moriya (DM) interaction plays a crucial role in a number of the most topical phenomena in magnetism, including the slow magnetic rotations found in Skyrmion lattices and cycloidal magnetoelectrics. The original formulation of the DM interaction related to the occurrence of ‘weak ferromagnetism’ in nominally antiferromagnetic materials such as FeBO_3 [1]. Unfortunately, in these archetypal twisted magnetic systems, the sign of the DM interaction has eluded experimenters because it affects only the phase of magnetic scattering, whereas experiments based on a single scattering mechanism determine only intensity (a manifestation of the famous “phase problem” of crystallography). This meant that the DM interaction in such weak ferromagnets could be determined in magnitude and axial direction, but not in sign.

Following the suggestion [2] that the sign of the DMI interaction might be determined by measuring interference between magnetic x-ray scattering and the pure quadrupole resonance at the iron K-edge (acting as a known reference wave), we carried out measurements of the (009) resonant quadrupole reflection on XMaS, using a small magnet to rotate the ferromagnet moment, which turned the antiferromagnetic structure and reversed the phase of the magnetic scattering signal (Fig. 4). This had the remarkable effect of causing a jump in the energy of the resonance due to the reversal of the interference conditions on the low and high energy side of the peak (Fig. 5). From the direction of the jump, we were able to determine the phase of the magnetic scattering and finally the sign of the DM interaction in globally centrosymmetric FeBO_3 [3]. Armed with these results, we could provide a thorough test of state-of-the-art first-principles calculations of the magnetic properties of this material, demonstrating that new computational techniques are able to correctly predict the fine details of the magnetic ground-state, and provide a platform for modelling other phenomena in which DM interactions play a key role.

[1] T. Moriya Phys. Rev. 120, 91–98 (1960).

[2] V. E. Dmitrienko *et al.* JETP Lett. 92, 383–387 (2010).

[3] V. E. Dmitrienko *et al.* Nature Physics 10, 202–206 (2014).

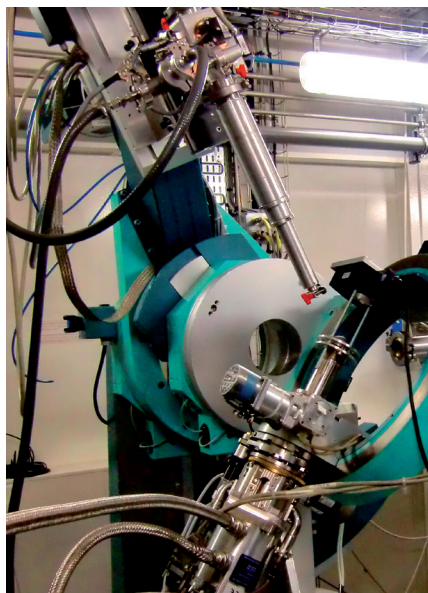


Fig. 4: The XMaS diffractometer supporting the sample cryostat and rotating magnet during the experiment.

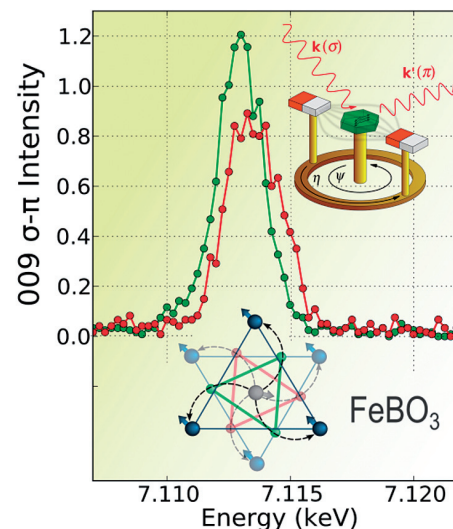


Fig. 5: The jump in the quadrupole resonance as the magnetic structure was rotated by 180 degrees. The relationship between the twisting of the magnetic moments and that of triangles of oxygen atoms between the iron planes is shown at the bottom.

Proximity induced magnetism in Pt/Co/Pt trilayers with heavy metal insertion layers

R. M. Rowan-Robinson, T. P. A Hase, L. Bouchenoire, S. D. Brown, A. T. Hindmarch, D. Atkinson – for more information contact D. Atkinson, Centre for material physics, Durham University, DH1 3LE, UK.

del.atkinson@dur.ac.uk

The study of current induced domain wall motion has attracted great interest due to potential applications in novel magnetic memory devices that combine fast write speeds with non-volatility. Recent investigations [1, 2] have shown that high domain wall velocities can be obtained in platinum/ferromagnet heterostructures with out-of-plane anisotropy for relatively low current densities. A variety of spin-orbit phenomena originating at this interface have been put forward as candidates to explain this behaviour, including the Rashba effect, spin Hall effect and the Dzyaloshinskii-Moriya interaction. Furthermore, the insertion of Au interlayers at this interface has been shown to have a large effect on domain wall mobility [3].

Platinum is well known to exhibit proximity induced magnetization (PIM) at the interface with a ferromagnet, therefore understanding the rich behaviour that occurs at this interface requires a deeper understanding of the PIM, in particular the length scale and mechanism of this interaction. This has been investigated through X-ray Resonant Magnetic Reflectivity (XRMR) of Pt/Co/Pt trilayers with the insertion of Au and Ir spacer layers of varying thickness between the top Co/Pt interfaces.

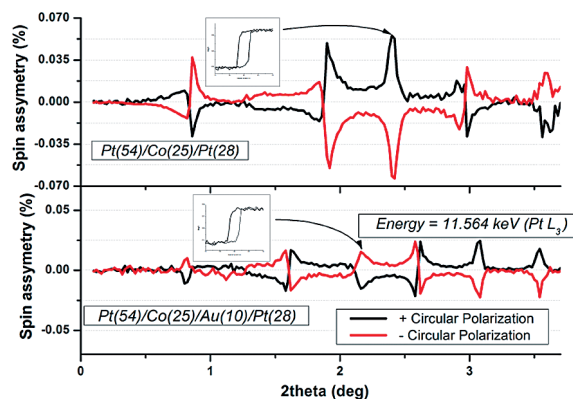


Fig. 6: Spin asymmetry ratio measured using XRMR. Insets show hysteresis loops measured at the Pt L3 edge by sweeping the field and measuring the spin asymmetry.

XRMR data was collected at the Pt L_{III} edge, using a phase retarder to produce circularly polarized light (Fig. 6). The polarization dependent scattering gives different reflectivity intensities dependent on the magnetization of the sample, from which the spin asymmetry ratio is calculated. This contains information on both the structural as well as the magnetic profiles.

The spin-asymmetry data was fitted using the GenX code [4], from which the scattering length density profiles (SLDs) were extracted (Fig. 7). These give detailed insight into the magnitude and structure of the magnetism at Co/Pt interface as a function of Au or Ir spacer layer (Fig. 8).

- [1] A. Brataas, Nature Nanotech., 8, 485 (2013).
- [2] S. Emori, U. Bauer, G. S. D. Beach, et al. Nature Mater., 12, 611 (2013).
- [3] K. Ryu, L. Thomas, S. Yang, S. Parkin, Nature Nanotech., 8, 527 (2013).
- [4] M. Björck and G. Andersson, J. Appl. Cryst., 40, 1174-1178 (2007).

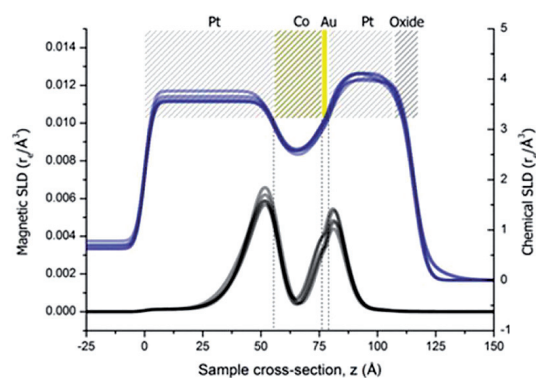


Fig. 7: Chemical (blue) and structural (black) SLD profiles extracted from fitting the spin asymmetry and reflectivity data for sample with a 2 Å Au insertion layer.

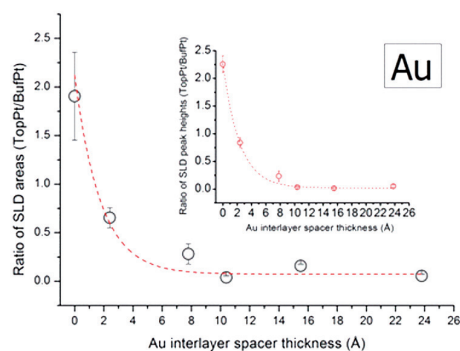


Fig. 8: Ratio of areas under magnetic SLD profile as a function of Au spacer. This demonstrates the rapid loss of moment on the top Pt layer relative to the buffer Pt layer as function of Au spacer. Inset: ratio of magnetic SLD peak heights as function of Au spacer.

Sweet Corrosion Scaling

G. R. Joshi, K. Cooper, J. Lapinski, D. L. Engelberg, O. Bikondoa, M. G. Dowsett, R. Lindsay – for more information contact R. Lindsay, Corrosion and Protection Centre, The School of Materials, The University of Manchester, Sackville Street, Manchester, M13 9PL, UK.

robert.lindsay@manchester.ac.uk

Within the oil industry, corrosion of carbon-steel pipelines, and other components, is a constant concern [1]. Internally, one of the primary issues is so called sweet corrosion, resulting from the dissolution of CO₂ into aqueous brines carried along with the oil. This process leads to the formation of H₂CO₃, a weak acid, which drives the corrosion of pipeline surfaces. Besides simple metal loss, solid corrosion products may also form, and adhere to the carbon-steel surface. This scaling can significantly reduce the rate of corrosion, and so is integral to material sustainability.

Typically, sweet corrosion scales are simply labelled as siderite (FeCO₃). Experimental data, however, indicate that these scales can be more complex, e.g. chukanovite (Fe₂(OH)₂CO₃) has been reported as a scale component [2]. One concern about such scale characterization is that most studies are undertaken *ex-situ*, i.e. following removal of the substrate from solution. This procedure may induce scale modification. To address this issue, we have developed an electrochemical cell (E-cell) suitable for electrochemical corrosion rate measurements and grazing incidence x-ray diffraction (GIXRD) from immersed samples. A photograph of the E-Cell



Fig. 9: Photograph of experimental setup on beam line.

mounted on the beam line is shown in (Fig. 9). The capability to make measurements at low dissolved oxygen concentrations and to vary the temperature of the solution have been incorporated into the design.

Electrochemical and *in-situ* GIXRD measurements were acquired from a pipeline carbon-steel (X65) sample immersed in CO₂-saturated 0.1M NaCl solution (pH = 6.8, T = 80°C). The corrosion rate reached a maximum of ~ 1.4 mm/y within the first hour, and then decreased over the next few hours, reaching a plateau at ~ 0.2 mm/y. During this period, there were also significant changes in the substrate termination, as indicated by the diffractograms in (Fig. 10). Besides substrate features (Fe), after 0.5 h of immersion a quite intense peak appears at 5.5°, which is assigned to a green rust (GR) carbonate [3]. This feature is not apparent in subsequent diffractograms, being replaced by features assigned to siderite and chukanovite. Over time, the intensities of the siderite peaks increase. Given that the initial development of this phase coincides with the reduction in corrosion rate, it is suggested that the siderite phase likely makes a significant contribution to controlling substrate corrosion. Latterly appearing peaks, attributed to iron oxides, are likely to be due to dissolution of some O₂ into the CO₂-saturated solution at longer immersion times.

We are grateful to BP for supporting this work through the BP-FTF program. GJ and KC acknowledge financial support from EPSRC through the Advanced Metallic Systems Centre for Doctoral Training.

- [1] M. B. Kermani, A. Morshed, Corrosion, 59, 659 (2003).
- [2] R. De Marco *et al.*, J. Electrochem. Soc., 152, B389 (2005).
- [3] P. Refait *et al.*, C. R. Geoscience 338, 476-487 (2006).

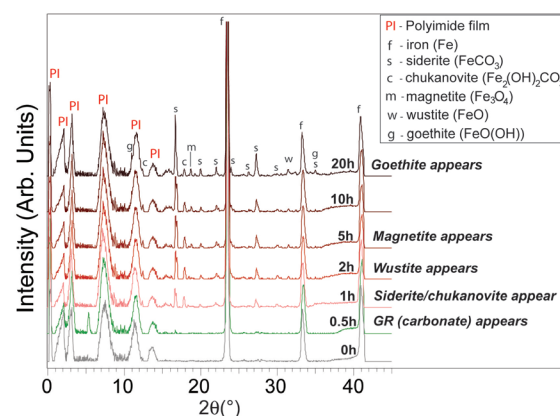


Fig. 10: Diffractograms, acquired as a function of immersion time, from X65 steel immersed in CO₂-saturated 0.1M NaCl solution (pH = 6.8, T = 80°C).

How molecules infiltrate ordered purple membrane films: An XRR study

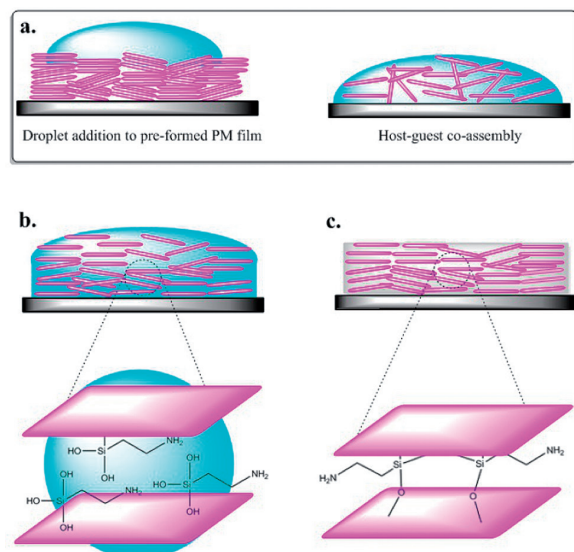
A. M. Collins, N. H. M. Kaus, O. Bikondoa, P. T. Cresswell, J. M. Bulpett, W. H. Briscoe and S. Mann – for more information contact A. Collins, Bristol Centre for Functional Nanomaterials (BCFN); or W. Briscoe, School of Chemistry, University of Bristol, UK.

andy.collins@bris.ac.uk; wuge.briscoe@bris.ac.uk

Intact sheets of purple membrane (PM), consisting of hexagonally packed trimeric arrays of the protein bacteriorhodopsin (bR) embedded within a lipid bilayer membrane 4.7 nm in thickness, can be readily isolated from the organism *Halobacterium salinarium*. PM sheets are typically 500–1000 nm in size, and of technological importance due to the photochromic and light harvesting properties of bR, which can pump protons from the cytoplasmic to extracellular side of the membrane under illumination [1]. In many technical applications, PM sheets are stacked by controlled sedimentation into mesostructured thin films that require some level of hydration to retain their proton-pumping functionality. Hybrid films formed by intercalating a guest material, in this instance an organosilane, with the PM sheets are more structurally robust than pure PM films, but intercalation can impact on protein functionality due to inhibition of water transport through the film [2]. Therefore, understanding the mechanism of intercalation and the role of hydration in the intercalation process and resultant film functionality are important aspects for the design and construction of hybrid PM films. *In-situ* X-ray reflectometry (XRR) was used to elucidate the formation mechanism of composite organosilane and PM films with ordered

lamellar structures [3]. Two methods of formulation were investigated (Fig. 11). In the first method, *guest infiltration*, a dilute aqueous solution of the organosilane precursor, aminopropyl silicic acid (APS), was placed atop a predeposited and ordered PM film. The droplet was allowed to infiltrate the PM film and dry to form a composite film. In the second method, *co-assembly*, the PM was dispersed into the aqueous APS solution and a droplet of the mixture was added to a silica substrate and allowed to dry to form the composite film.

A PM control film had a lamellar spacing of 4.7 nm, as observed by XRR. If this film was treated with water alone then the observed structure was lost. Subsequent air-drying induced re-stacking of the lipid/protein membranes, however, with retention of a 2–3 nm hydration layer within the interlamellar spaces. Complete drying of the PM control films resulted in the disappearance of reflections correlating to ordered PM layers swollen with water and the re-emergence of the 4.7 nm lamellar spacing. Similarly, our results show that addition of an aqueous solution of guest APS molecules to a dried preformed PM film followed the same drying mechanism except that upon formation of the interstitial hydration layers the guest organosilane precursor underwent hydrolysis and condensation. In completely dry composite organosilane PM films a lamellar spacing of 5–6 nm was observed. From this work we believe that the hydration layer is necessary for the intercalation of APS molecules into the PM film, and their subsequent condensation and retention as nano-thin inorganic lamellae within the composite mesostructure after drying. It was also possible to elucidate the ordering in the PM film and our results indicate that the intercalated nanocomposites prepared from preformed PM films exhibited a higher degree of ordering than those produced by co-assembly.



[1] D. Oesterhelt *et al*, *Nature*, 233, 149–152 (1971).

[2] A. M. Collins *et al*, *J. Mater. Chem*, 20, 9037–9041 (2010).

[3] N. H. M. Kaus *et al*, *J. Mater. Chem. C*, 2, 5447–5452 (2014).

Fig. 11:

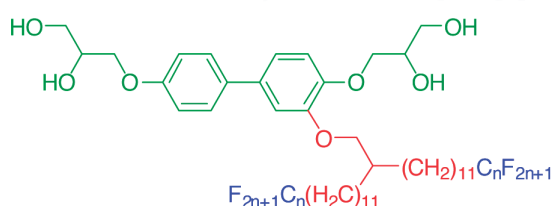
(a): A schematic showing the two methods of composite film preparation: a droplet containing APS solution added to a preformed PM film and host-guest co-assembly from mixing the components together prior to drying. (b): The transient phase of intercalation in which the PM lamellar structure becomes disordered and swollen with the solution. (c): Upon complete dehydration, the APS is condensed into a solid organosilane interstitially between PM layers.

Skeletal Cubic, Lamellar, and Ribbon Phases of Bundled Thermotropic Bolapolyphiles

F. Liu, M. Prehm, X. B. Zeng, C. Tschierske, G. Ungar – for more information contact G. Ungar, Department of Materials Science and Engineering, University of Sheffield, Sheffield, S1 3JD, UK.

g.ungar@shef.ac.uk

A series of T-shaped polyphilic molecules composed of a rigid linear aromatic core with a polar glycerol group at each end and one “swallow-tail” partially fluorinated side-chain of different lengths n (see chemical formula), were synthesized and their liquid crystalline (LC) phases were investigated by small-angle grazing incidence X-ray scattering (GISAXS) on BM28, as well as by other techniques [1].



Similar molecules with smaller side-groups show a remarkable series of honeycomb-like LC phases with the aromatic rods as the “wax” and the side-chains as “honey”. However, here we find that, as the side-groups increase, the honeycomb cells open up, resulting in an alternating layer structure (Fig. 12: g). As temperature is raised, the flexible side-chains expand faster than the rigid cores, and the growing mismatch results in the aromatic layers (green) being shredded into parallel ribbons (symmetry $c2mm$). Interestingly, the molecules are highly aligned along the ribbon axis, forming a nematic LC phase self-confined within these 2-3 nm wide channels (Fig. 12: h).

As the temperature is increased further, birefringence is lost (Fig. 12: c) as the structure becomes cubic ($Ia\bar{3}d$, Fig. 12: i). Unlike in any other “double gyroid” bicontinuous phase, the molecular rods are parallel to the segments of the interpenetrating networks. This new mode of molecular self-assembly promises potential 3-d semiconductors for applications such as organic photovoltaic materials.

[1] F. Liu, M. Prehm, X. B. Zeng, C. Tschierske, G. Ungar, J. Am. Chem. Soc. 136, 6846–6849 (2014).

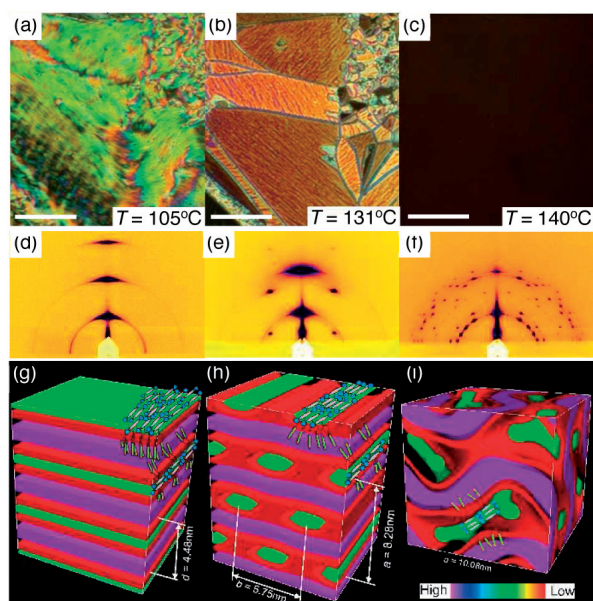


Fig. 12:

(a-c): Textures as seen between crossed polarizers in the (a) lamellar phase at 105 °C; (b): ribbon phase at 131 °C and (c): Cubic phase at 140 °C. Scale bar: 50 μm .
 (d-f): GISAXS patterns from a thin film in the (d) lamellar, (e) ribbon and (f) cubic $Ia\bar{3}d$ phase.
 (g-i): Histogrammatic electron density maps with added schematic molecules for (g) lamellar, (h) ribbon, and (i) cubic phase. Discrete solid colours are allocated to three different density ranges, purple for the highest, green for the middle and red for the lowest; they correspond roughly to chemical group colours in the chemical formula above.

Superspreading fluids investigated by GISAXS

D. S. Martin, K. Williams, O. Bikondoa, D. Dennis and V. Bertola – for more information contact D. S. Martin, Department of Physics, University of Liverpool, Liverpool, L69 7ZE, UK.

David.Martin@liverpool.ac.uk

Placing a droplet of water onto a low-energy hydrophobic surface results in the well-known “pearling” effect: the droplet remains intact with minimal or no wetting of the surface. However, it is often desirable in many applications for water-based fluids to spread rapidly and form a film over the substrate. Commercial processes involving coatings and sprays, pharmaceutical manufacturing and agricultural processes such as water-born pesticide treatments would find enhanced spreading highly desirable, with potential ecological and economic benefits in minimising usage of water and pesticides. In addition to these applications, enhanced spreading is an interesting fundamental problem of fluid dynamics that is currently poorly understood.

To encourage spreading, the surface tension of the liquid may be reduced by adding small amounts of surfactants. A more dramatic approach that achieves a rapid and effective spreading over hydrophobic surfaces involves the use of trisiloxane-based “superspreader” surfactants. This “superspreading” behaviour cannot be explained in terms of surface tension reduction [1,2].

A model has been proposed that attempts to explain the difference between superspreading and non-superspreading surfactants (which can appear chemically to be very similar) in terms of either

micelle crystallisation or mono/bi-layer formation [1]. One of the aims of our experiment was to explore if superspreader molecules form ordered structures at the fluid/substrate interface and if so, the nature and extent of the ordering. We were encouraged by the previous observation that ordered macromolecular structures near a moving contact line affect significantly the wetting behaviour of dilute solutions of flexible polymers [3].

We have used grazing incidence small angle x-ray scattering (GISAXS) at XMaS to investigate the dynamic wetting behaviour of superspreader and non-superspreader solutions on various polymer substrates. By comparing a superspreader surfactant to a non-superspreading surfactant we could probe differences in hypothesised micellar-substrate and lamella-substrate structures. We are currently in the process of analysing the data and present here a few preliminary findings.

We observed diagonal flares in the GISAXS data as the droplet advanced across the x-ray beam position on the substrate (Fig. 13). These flares provide a measure of the liquid free surface angle as a function of spreading time. On closer inspection, some of the flares show a regular banding structure which indicates a periodicity of the order of 10 nm. Preliminary analysis of our data suggests the presence of molecular layers ordered in the out-of-plane direction, rather than in-plane-ordered micellar structures. With further analysis of the data we expect to discriminate between the two proposed models.

[1] J. Venzmer, *Curr Opin Colloid Interface Sci* 16, 335 (2011).

[2] R. M. Hill, *Curr Opin Colloid Interface Sci* 3, 247 (1998).

[3] M. I. Smith and V. Bertola, *Phys. Rev. Lett.* 104, 154502 (2010).

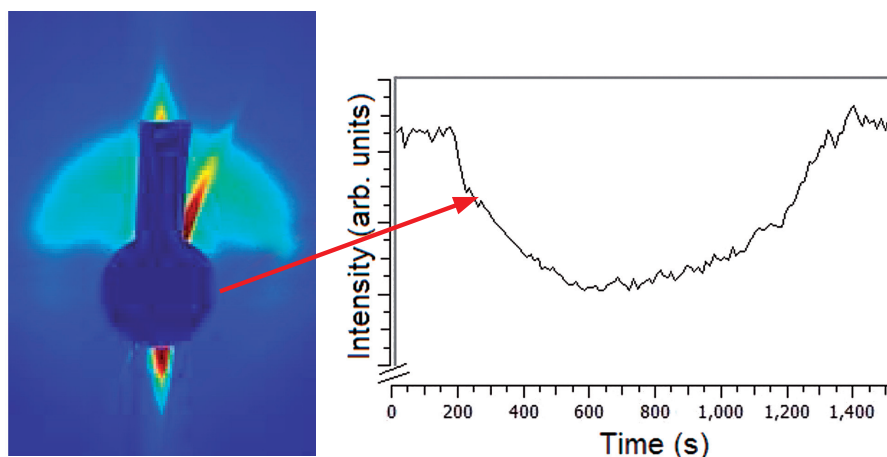


Fig. 13:
Left: GISAXS image from a sequence following the superspreading of a droplet on a polypropylene substrate.
Right: X-ray intensity changes with time as the droplet spreads across the beam and subsequent evaporation.

Crystal Structure of Conjugated Polymers: a Combined Scattering and Atomistic Simulation Approach

A. A. Y. Guilbert, S. Lilliu, J. E. Macdonald and J. Nelson – for more information contact A. A. Y. Guilbert, Department of Physics, Imperial College London, London SW7 2AX, UK.

a.guilbert09@imperial.ac.uk

Organic photovoltaics (OPV) is a promising technology with the potential to deliver a cheap, lightweight, flexible and large area solution for niche applications in electricity generation. The device performance is strongly affected by the microstructure of the polymer-fullerene blends, which in turn is influenced by the processing conditions and the chemical structure of the blend components.

We studied the influence of the heteroatom (carbon or silicon) that links the side chains, that solubilise the polymer, to the cyclopentadithiophene unit in PCPDTBT. **Fig. 14** displays the grazing incidence wide angle X-Ray scattering (GIWAXS) pattern for the two molecules. The silicon analogue, which displays a better defined diffraction pattern, shows a higher tendency to crystallise than the carbon analogue. From the patterns we notice that the crystals of the two analogues are oriented differently with respect to the substrate. By substituting the carbon atom with a silicon atom, the π - π stacking distance – which is the distance between the flat, conjugated backbones of the polymers when stacked on top of one another cofacially (**Fig. 15**) – decreases at the cost of increasing the lamellar stacking distance.

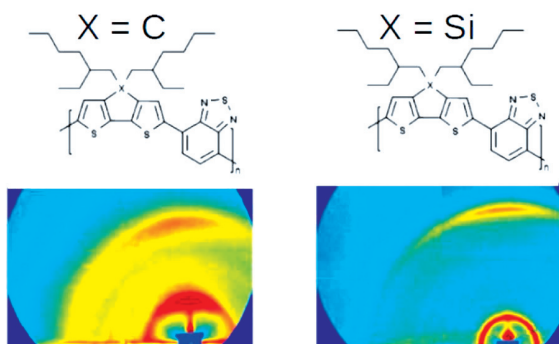


Fig. 14: GIWAXS 2D diffraction pattern of C-PCPDTBT and Si-PCPDTBT.

To bridge the gap between chemical structure and crystal structure, we combine GIWAXS with molecular dynamics simulations (MD). From the quantum chemical calculations, we can determine the conformation of the cyclopentadithiophene and benzothiadiazole units and that the side chains of the silicon analogue are more flexible. We build a crystal structure with polymers with a π -electron stack featuring a two-fold axis parallel to the main chain axis simply translated to create lamellar stack (**Fig. 15**). Then, we scan the energy surface of this structure when varying the π - π stacking and lamellar stacking distances (for each configuration, the side chains are relaxed by performing a MD simulation at 300 K in a NPT ensemble, as shown in **Fig. 15**) and study the contributions of both backbones and side chains.

We propose that the greater side chain flexibility of the silicon bridged polymer enables that material to find the minimum with the shorter π - π stacking distance, which should enable improved hole transport, leading to the higher hole mobilities that have been observed and to easier photocurrent generation in a solar cell. These studies confirm that structural characterisation using GIWAXS combined with molecular modelling can help to explain the difference in performance of organic electronic materials in terms of their chemical structure and packing tendency.

For further details, see A. A. Y. Guilbert *et al.*, *Chemistry of Materials*, 26, 1226-1233, (2014).

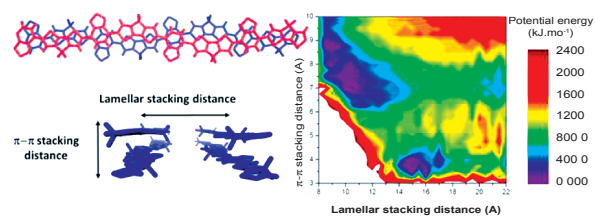


Fig. 15: Structure and calculated potential energy surface (PES) for C-PCPDTBT. The step size is 0.25 Å for the π - π stacking and 0.5 Å for the lamellar stacking.

Structural evolution of photo-polymerised dimethacrylate resin systems

S. Sirovica, O. Addison, M. W. A. Skoda, P. Thompson, W. Palin, R. A. Martin – for more information contact R. A. Martin, School of Engineering, Aston University, Birmingham, B4 7ET, UK or O. Addison, School of Dentistry, University of Birmingham, B4 6NN, UK.

r.a.martin@aston.ac.uk; o.addison@bham.ac.uk

Over 370 million dental mercury amalgam fillings are fitted in Europe annually [1]. Yet its removal as a clinical restorative treatment option is imminent in several European nations due to environmental and health concerns. The most promising alternative class of restorative material are resin based composites (RBCs) consisting of a dimethacrylate polymer matrix and inorganic filler particles. RBCs are “demand set” by light activation of a photo-initiator species embedded within the resin to initiate polymerisation, however they typically demonstrate inferior clinical performance and lifetime in comparison to amalgam and are highly sensitive to the curing regime [2]. Despite extensive mechanical characterisation of these polymers, the impact of curing rate on the resultant molecular structure has yet to be directly elucidated. Time resolved small angle X-ray scattering measurements were undertaken at XMaS to determine the structural changes within the forming polymer network as a function of polymerisation rate. Samples were formulated from bisphenol A-glycidyl

methacrylate and triethylene glycol dimethacrylate monomers for 60:40 and 40:60 wt. % blends, incorporating the fast and slow acting initiators Lucirin TPO and Camphorquinone respectively.

The polymerisation reaction was found to alter the short range conformation (Fig. 16) and order within the methacrylate functional end groups where the monomer chains react. Fig. 17 shows how increasing the polymerisation rate through a combination of high light intensity and a reactive photo-initiator species (TPO) correlates to a larger degree of molecular extension. The largest extensions were observed for samples rapidly photo-cured, whilst the smallest extensions correlated with the slower curing rates. Resins polymerised rapidly also demonstrated a subsequent relaxation (Fig. 17). Rapid polymerisation therefore created greater effective free volume and induced greater molecular strain, which the system attempted to alleviate through this relaxation. Furthermore, on decreasing the polymerisation rate, a higher degree of short range order was observed; approximately double that seen for fast cured resins.

Our results have demonstrated that the curing regime employed by a dentist when photo-setting a resin filling can significantly influence the resultant polymer structure and molecular strain within the material.

[1] European Commission, DG ENV – Final Report, (2012).

[2] R. Hickel, *et al.* Am J. Dent, 18:198-2, (2005).

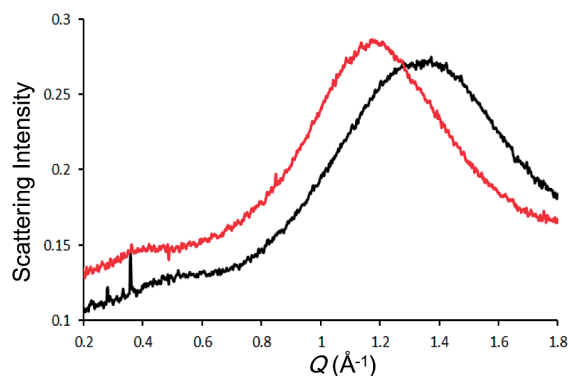


Fig. 16: Diffraction pattern on the monomer blend (black) and the blend after photocuring for 6 seconds (red). A shift to lower Q during polymerisation indicates the extension within the methacrylate end group.

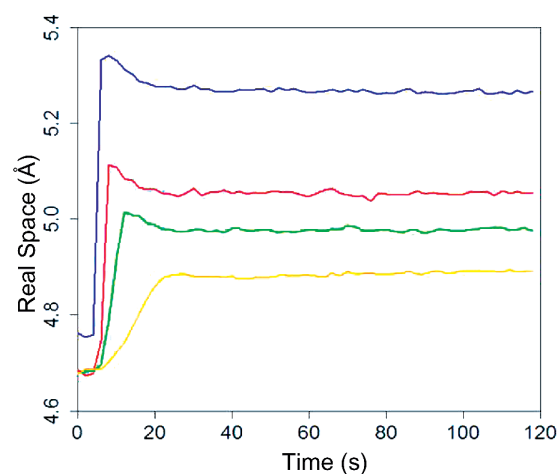


Fig. 17: Molecular extension for CQ (green, orange) and TPO (blue, red) initiated resins at high and low irradiances during polymerisation.

Silver corrosion in real time

R. Wiesinger, R. Grayburn, M. Dowsett, P. J. Sabbe, P. Thompson, A. Adriaens and M. Schreiner – for more information contact M. Dowsett, Department of Physics, University of Warwick, Coventry, CV4 7AL, UK.

m.g.dowsett@warwick.ac.uk

From its veneration above gold in ancient Egypt to modern applications such as the prevention of bacterial growth in clothing and wound dressings (exploiting an antibacterial property known since at least the 8th Century) silver and its alloys remain a central part of human technology, commerce and art after 8 to 10 millennia of use. Yet, the corrosion of silver is a complex phenomenon and is not well understood; fundamental research into the chemistry occurring on surfaces exposed to the environment is needed so that material degradation can be controlled. The most common corrosion products (the sulfides) are black, but we expect to see silver with a lustrous surface often with intricate chasing (**Fig 18**). Thus, for example, silver museum artefacts, have, been repeatedly cleaned and polished over 100s or even 1000s of years, leading to serious loss of surface detail and other damage [1]. In these experiments [2] we examined, in real time, the early stages of the corrosion of silver exposed to the anthropogenic gases H_2S and O_3 at various levels of relative humidity (RH). A particular goal was to look for synergistic effects in gas mixtures to closer approach the real environment. Experiments were carried out in an electrochemical /environmental cell (eCell) developed at the universities of Ghent (BE) and Warwick (UK) [3] fed by a gas mixing unit designed and built at the Academy of Fine Arts in Vienna [4]. Synthetic air containing 500 ppb O_3 and/or 500 ppb or 10 ppm H_2S at 50% or 90% RH was



Fig. 18: Heavily engraved silver chalice in the Liechtenstein Museum, Vienna, with permission.

blown through the eCell which contained a high purity silver coupon. In experiments lasting 12–24 hours SR-XRD patterns were recorded every 10 min using the Mar CCD 165 camera with an acquisition time per image of 20 s. Images were reduced to 1D patterns and trends in peak area over time were extracted using the esaProject package.

Overall the effects were neither linear, nor monotonic and the patterns reveal different behaviour for different compounds coexisting on the same surface, changes in rates of corrosion over time, and a strong dependence of the rate of corrosion on the gas mixture. For example, the growth of silver oxides in O_3 at 50% RH was shown to proceed via cubic Ag_2O for 3 hours or so then AgO related reflections appear followed by more complex oxides after 10 hours (polymorphic AgO , Ag_2O_3 and Ag_3O_4). The total coverage is still increasing rapidly after 24 hours. Conversely, when O_3 is replaced by H_2S at the same level (**Fig 19**), a fresh coupon shows little evidence of corrosion on the same timescale. However, if O_3 is added to the mix after 12 hours, a very rapid increase in coverage of both sulfides and oxides is observed. We conclude that at concentrations close to those found in city centres, synergistic effects between O_3 and H_2S lead to greatly accelerated rates of corrosion.

- [1] C. Leygraf, T. E. Gradel, *Atmospheric Corrosion*, John Wiley & Sons, New York, (2000).
- [2] R. Wiesinger *et al.*, presented at SR2A, Paris 2014 and submitted to JAAS.
- [3] M. Dowsett, A. Adriaens, *Anal. Chem.* 78 3360-3365 (2006.)
- [4] R. Wiesinger, M. Schreiner and C. Kleber, *Appl. Surf. Sci.*, 256 2735-2741 (2010).

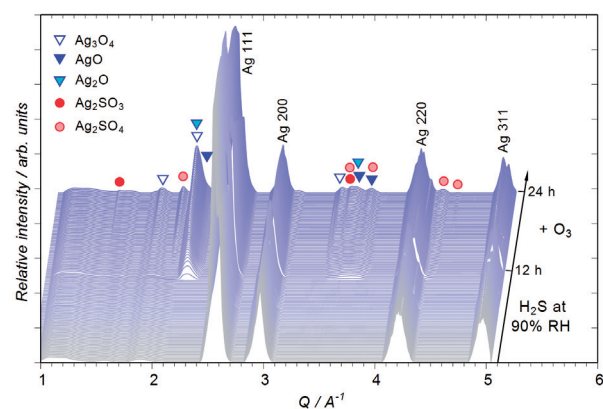


Fig. 19: Waterfall plot of extracted and normalized SR-XRD patterns for two part experiment with initial exposure to H_2S at 90% RH with the addition of O_3 after 12 hours. Note the rapid appearance of corrosion peaks upon the addition of O_3 .

➔ Please note

Some of the experimental reports in the previous pages are as yet unpublished. Please email the contact person if you are interested in any of them or wish to quote these results elsewhere.

➔ Our web site

This can be found at: www.xmas.ac.uk and contains the definitive information about the beamline, future and past workshops, press articles and Key Performance Indicators (KPIs). You can also follow what happens on the beamline every week on **Twitter @XMaSBeam**.

➔ Living allowances

These are € 70 per day per beamline user — the equivalent actually reimbursed in pounds sterling. XMaS will support up to 3 users per experiment. For experiments which are user intensive, additional support may be available. The ESRF hostel still appears adequate to accommodate all our users, though CRG users will always have a lower priority than the ESRF's own users. Do remember to complete the "A-form" when requested to by the ESRF, as this is used for hostel bookings, site passes and to inform the safety group of attendees.

➔ Beamline people

● **Beamline Responsible** – Simon Brown (sbrown@esrf.fr), in partnership with the Directors, oversees the activities of the user communities as well as the programmes and developments that are performed on the beamline. He is also the beamline Safety Representative.

● **Beamline Coordinator** – Laurence Bouchenoire, (boucheno@esrf.fr), looks after beamline operations and can provide you with general information about the beamline, application procedures, scheduling, etc. Laurence should normally be your first point of contact.

● **Beamline Scientists** – Simon Brown (sbrown@esrf.fr), Oier Bikondoa (oier.bikondoa@esrf.fr), Didier Wermeille (didier.wermeille@esrf.fr) and Laurence Bouchenoire (boucheno@esrf.fr) are Beamline Scientists and will provide local contact support during experiments. They can also assist with queries regarding data analysis and software.

● **Postdoctoral Research Associate** – Sean McMitchell (sean.mcmitchell@esrf.fr) is associated with the Nanostrain project (<http://www.piezoinstitute.com>). He provides support for in situ interferometry and electrical measurements on the beamline and on the offline facilities.

● **Technical Support** – Paul Thompson (pthomps@esrf.fr) is the contact for instrument development and technical support. He is assisted by John Kervin (jkervin@liv.ac.uk), who is based at Liverpool University, provides further technical back-up and spends part of his time on-site at XMaS.

● **Project Directors** – Chris Lucas (clucas@liv.ac.uk) and Tom Hase (t.p.a.hase@warwick.ac.uk) continue to travel between the UK and France to oversee the operation of the beamline. Malcolm Cooper (m.j.cooper@warwick.ac.uk) remains involved in the beamline operation as an Emeritus Professor at the University of Warwick. Kayleigh Lampard (Kayleigh.Lampard@warwick.ac.uk) is now the principal administrator on the project and is

based in the Department of Physics at Warwick. All queries regarding expenses claims, etc. should be directed to her. Linda Fielding (linda.fielding@liv.ac.uk) is the administrator at the University of Liverpool.

The Project Management Committee

The current membership of the committee is as follows:

- P. Hatton (chair), University of Durham
- Simon Crook, EPSRC
- A. Boothroyd, University of Oxford
- R. Cernik, University of Manchester
- K. Edler, University of Bath
- B. Hickey, University of Leeds
- S. Langridge, ISIS, Rutherford Appleton Laboratory
- C. Nicklin, Diamond Light Source
- W. Stirling, Institut Laue Langevin

In addition to the above, the directors, the chair of the PRP and the beamline team are in attendance at the meetings which happen twice a year.

➔ The Peer Review Panel

The current membership of the panel is as follows:

- Elizabeth Blackburn, University of Birmingham
- Wuge Briscoe, University of Bristol
- Carsten Detlefs, ESRF
- Yvonne Gründer, University of Liverpool
- Roger Johnson, Oxford University
- Sean Langridge, ISIS
- Jorge Quintanilla, University of Kent
- Richard Walton, University of Warwick
- John Webster, ISIS

In addition either Chris Lucas or Tom Hase attends the meetings in an advisory role.

➔ Housekeeping!!

At the end of your experiment samples should be removed, tools, etc. returned to racks and unwanted materials disposed of appropriately. When travel arrangements are made, therefore, please allow additional time to effect a tidy-up.

➔ PUBLISH PLEASE!... and keep us informed

Although the list of XMaS papers is growing we still need more of those publications to appear. We ask you to provide Laurence Bouchenoire with the reference. Note that the abstract of a publication can also serve as the experimental report!

➔ IMPORTANT!

When beamline staff have made a significant contribution to your scientific investigation you may naturally want to include them as authors. Otherwise we ask that you add an acknowledgement, of the form:

"This work was performed on the EPSRC-funded XMaS beamline at the ESRF, directed by C.A. Lucas, T.P.A. Hase and M.J. Cooper. We are grateful to S.D. Brown, O. Bikondoa, D. Wermeille, L. Bouchenoire and P. Thompson for their invaluable assistance, and to K. Lampard and J. Kervin for additional support."

How to apply for synchrotron beam time ?

→ Beamline Operation

The XMaS beamline at the ESRF has some 174 days of synchrotron beam time available each year for UK user experiments, after deducting time allocated for ESRF users, machine dedicated runs and maintenance days. During the year, two long shut-downs of the ESRF are planned: 4 weeks in winter and 4 weeks in summer. At the ESRF, beam is available for user experiments 24 hours a day.

→ Applications for Beam Time

Two proposal review rounds are held each year. **Deadlines for applications to make use of the mid-range facility (CRG) time are normally, 1st April and 1st October** for the scheduling periods August to end of February, and March to July, respectively. Applications for Beam Time must be submitted electronically following the successful model used by the ESRF. Please consult the instructions given in the ESRF web page:

www.esrf.eu

Follow the links “**User Portal**” under “**quick links**”.

Enter your surname and password and select:

“**Proposals/Experiments**”.

Follow the instructions carefully — you must choose “CRG Proposal” and “XMAS-BM28” at the appropriate stage in the process. A detailed description of the process is always included in the reminder that is emailed to our users shortly before the deadline – for any problems contact L. Bouchenoire (boucheno@esrf.fr). Technical specifications of the beamline and instrumentation available are described in the XMaS web page (www.xmas.ac.uk).

■ When preparing your application, please consider that access to the mid-range facility time is only for UK based researchers. Collaborations with EU and international colleagues are encouraged, but the proposal must be led by a UK based principal investigator and it must be made clear how the collaborative research supports the UK science base. Applications without a robust link to the UK will be rejected and should instead be submitted directly to the ESRF.

■ All sections of the form must be filled in. Particular attention should be given to the safety aspects, and the name and characteristics of the substance completed carefully. Experimental conditions requiring special safety precautions such as the use of electric fields, lasers, high pressure cells, dangerous substances, toxic substances and

radioactive materials, must be clearly stated in the proposal. Moreover, any ancillary equipment supplied by the user must conform to the appropriate French regulations. Further information may be obtained from the ESRF Experimental Safety Officer, tel: +33 (0)4 76 88 23 69; fax: +33 (0)4 76 88 24 18.

■ Please indicate your date preferences, including any dates that you would be unable to attend if invited for an experiment. This will help us to produce a schedule that is satisfactory for all.

■ It is anticipated that the offline x-ray and electrical measurement facilities will become available to users in the spring of 2015. If you require access to these facilities in conjunction with your synchrotron proposal, please indicate this in the scientific case section together with justification and the number of days required.

■ An experimental report on previous measurements must be submitted. Applications will not be considered unless a report on previous work is submitted. These should also be submitted electronically, following the ESRF model. The procedure for the submission follows that for the submission of proposals — again, follow the instructions in the ESRF’s web pages carefully. Reports must be submitted within 6 months of the experiment. Please also remember to fill in the end of run survey on completion of your experiment, which is available on the beamline website.

■ The XMaS beamline is available for one third of its operational time to the ESRF’s user community. Applications for beamtime within that quota should be made in the ESRF’s proposal round - Note: their deadlines are earlier than for XMaS! - 1st March and 1st September. Applications for the same experiment may be made both to XMaS directly and to the ESRF. Obviously, proposals successfully awarded beamtime by the ESRF will not then be given beamtime additionally in the XMaS allocation.

→ Assessment of Applications

The Peer Review Panel for the UK-CRG considers the proposals, grades them according to scientific excellence, adjusts the requested beam time if required, and recommends proposals to be allocated beam time on the beamline. Proposals which are allocated beam time must in addition meet ESRF safety and XMaS technical feasibility requirements. Following each meeting of the Peer Review Panel, proposers will be informed of the decisions and some feedback provided.

HUBER
Diffraction and Positioning Equipment

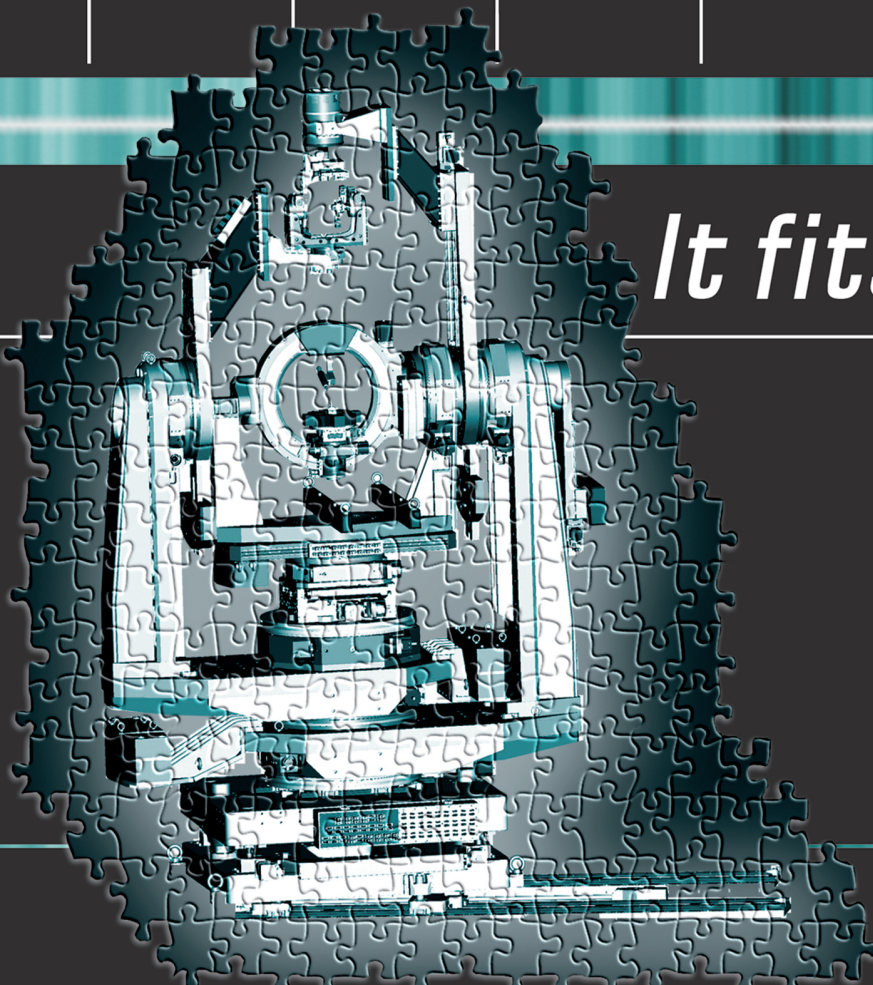
It fits

- X-Ray Diffractometers and Cameras
- Multiaxis Goniometers for X-Ray-, Synchrotron- and Neutron Facilities
- Monochromators
- Positioning Devices for Various Environments
- Electronics
- Accessories

We make the Best of your Beam

Sommerstrasse 4
D-83253 Rimsting, Germany

www.xhuber.com
info@xhuber.com



is an EPSRC sponsored project

XMaS, ESRF, 71 avenue des Martyrs, 38000 Grenoble, France
Tel: +33 (0)4 76 88 25 80; Fax: +33 (0)4 76 88 24 55 – web page : www.xmas.ac.uk – email: bouchenoire@esrf.fr